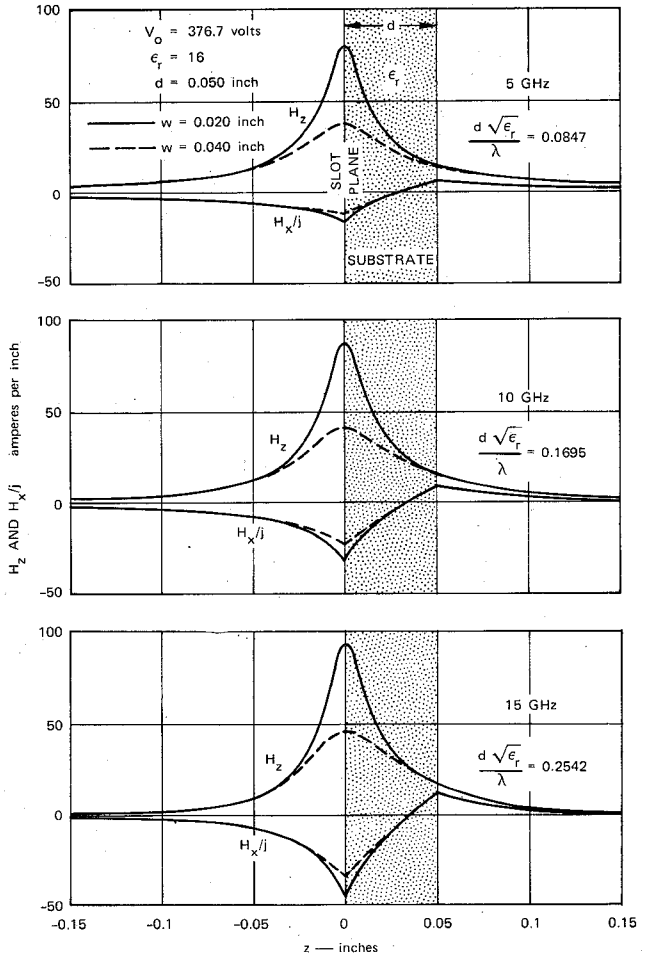

Fig. 3. Graphs of H_z and H_x/j along z axis for several slot widths and frequencies.

sheet, a TEM wave will propagate with $H_z=\sqrt{\epsilon_r'}E_y/\eta$. A comparison of the mode-summation equations for E_y and H_z on the air side of the slot yields $H_z=(\lambda/\lambda')E_y/\eta$, while a comparison for the substrate side yields the same relation when z is near zero (or for all z, if $d=\infty$). Therefore, we are justified in using the following quasi-static formula

$$H_z=\frac{\sqrt{\epsilon_r'}}{\eta}E_y, \qquad \epsilon_r'=\left(\frac{\lambda}{\lambda'}\right) \tag{12}$$

to compute H_z close to the slot.

Quasi-static H_z is plotted as a dotted curve in Fig. 2, and lies in a reasonable relationship to the solid curve. The two curves can clearly be blended together by transitions to yield a single curve of good accuracy. This was done in the field graphs in Fig. 3.

Application of Maxwell's equation $\nabla\times\boldsymbol{H}=j\omega\epsilon\boldsymbol{E}$ yields

$$H_x=H_x(z_1)-\frac{j2\pi}{\lambda'}\left[1-\epsilon_r\left(\frac{\lambda'}{\lambda}\right)^2\right]\int_{z_1}^{z}H_z\,dz. \tag{13}$$

To compute H_x versus z, the best choice of z_1 is at a point in the air region $z\leq 0$ where both the mode-summation and quasi-static solutions for H_z have good accuracy. In Fig. 2, $z_1=-0.016$ in is a suitable choice. The interval along the z axis, from $z=z_1$ to $z=0.010$ in is a region of good accuracy for the quasi-static solution. Substitution of (11) and (12) in (13) gives the following for H_x versus z with $y=0$:

$$H_x=H_x(z_1)-\frac{j2V_0}{\lambda\eta}\left[\left(\frac{\lambda}{\lambda'}\right)^2-\epsilon_r\right]\cdot\left[\sinh^{-1}\left(\frac{2z}{w}\right)-\sinh^{-1}\left(\frac{2z_1}{w}\right)\right]. \tag{14}$$

In using (14), evaluate $H_x(z_1)$ from the mode-summation formula (1). At $z\leq 0$, let $\epsilon_r=1$; at $z\geq 0$, let ϵ_r equal the substrate value. Equation (14) for H_x is plotted as a dotted curve in Fig. 2. Blending the solid and dotted curves to obtain a corrected curve is a simple matter.

Fig. 3 shows computed curves of H_z and H_x/j versus z for $y=0$, $V_0=376.7$ V, $\epsilon_r=16$, $d=0.050$ in, $w=0.020$ and 0.040 in, and $f=5$, 10, and 15 GHz. The mode-summation formulas were modified near $z=0$ by the quasi-static formulas, as described in the preceding paragraphs. Above 15 GHz, $d\sqrt{\epsilon_r}/\lambda>0.25$ and interference from surface waves is possible. Because H_z is real and H_x imaginary, the magnetic field is elliptically polarized in the z and x plane. The axial ratio is $\overline{AR}=|H_z/H_x|$. Note that $|H_z/H_x|$ is greater than one for all z values, and hence the condition $\overline{AR}=1$ for circular polarization is not met at any point. The curves show that the closest approach to circular polarization occurs at the largest w and the highest f. For example, with $w=0.040$ in and $f=15$ GHz, $\overline{AR}=1.351$ and 1.472 at the $z=0$ and $z=d$ surfaces of the substrate, respectively. Between $z=0$ and $z=d$ in the substrate, $\overline{AR}$ rises and is infinite at about $z=0.7d$. The point $\overline{AR}=\infty$ occurs where H_z/j passes through zero. Since the sign of H_z/j changes at this point, the direction of rotation of the elliptical polarization vector also changes.

References

[1] S. B. Cohn, "Slot line on a dielectric substrate," *IEEE Trans. Microwave Theory Tech.*, vol. MTT-17, pp. 768–778, Oct. 1969.
[2] E. A. Mariani, C. P. Heinzman, J. P. Agrios, and S. B. Cohn, "Slot line characteristics," *IEEE Trans. Microwave Theory Tech.*, vol. MTT-17, pp. 1091–1096, Dec. 1969.
[3] G. H. Robinson and J. L. Allen, "Slot line application to miniature ferrite devices," *IEEE Trans. Microwave Theory Tech.*, vol. MTT-17, pp. 1097–1101, Dec. 1969.
[4] F. C. de Ronde, "A new class of microstrip directional couplers," in *1970 G-MTT Symp. Dig.*, pp. 184–189, 1970.
[5] E. A. Mariani and J. P. Agrios, "Slot line filters," in *1970 G-MTT Symp. Dig.*, pp. 190–195, 1970.
[6] J. K. Hunton and J. S. Takeuchi, "Recent developments in microwave slot line mixers and frequency multipliers," in *1970 G-MTT Symp. Dig.*, pp. 196–199, 1970.
[7] H. J. Schmitt, "Fundamentals of microwave integrated circuits," in *Proc. Swedish Seminar on New Microwave Components* (Stockholm, Sweden), 1970.
[8] S. B. Cohn, "Sandwich slot line," *IEEE Trans. Microwave Theory Tech.* (Corresp.), vol. MTT-19, pp. 773–774, Sept. 1971.
[9] E. G. Cristal, R. Y. C. Ho, D. K. Adams, S. B. Cohn, L. A. Robinson, and L. Young, "Microwave synthesis techniques," Stanford Res. Inst., Menlo Park, Calif., Contract DAAB07-68-C-0088, SRI Project 6884, Final Rep., Nov. 1969.
[10] D. Chambers, S. B. Cohn, E. G. Cristal, and L. Young, "Microwave active network synthesis," Stanford Res. Inst., Menlo Park, Calif., Contract DAAB07-70-C-004, SRI Project 8245, Semiannu. Rep., June 1970.
[11] E. Weber, "Mapping of fields," in *Electromagnetic Fields*, vol. I. New York: Wiley, 1950, p. 340, eq. (38); also p. 304, eq. (7).

A Highly Stabilized K_a-Band Gunn Oscillator

S. NAGANO AND S. OHNAKA

***Abstract*—The construction and experimental results of a highly stabilized K_a-band Gunn oscillator are described. The frequency stability is 3×10^{-5} at 25 GHz over the temperature range from 0 to 50°C. An output power of more than 20 mW has been obtained in the frequency range up to 30 GHz. The frequency-saturation effect is also described.**

The Gunn diode is one of the most promising devices for local oscillator applications in microwave and millimeterwave communication receivers because of their low AM noise. However, the FM noise or the short-term stability is larger than that of a reflex klystron, and the long-term stability is also worse. The frequency stability of the ordinary Gunn oscillators and the required value of the stability in the communication systems are in the order of 10^{-3} and 10^{-5}, respectively, over the temperature range from 0 to 50°C. The stability can be improved by increasing the stored energy in the oscillator cavity without any sacrifice of the output power. This can be achieved

Manuscript received March 18, 1971; revised May 19, 1971.
The authors are with the Nippon Electric Company, Central Research Laboratories, Kawasaki, Japan.

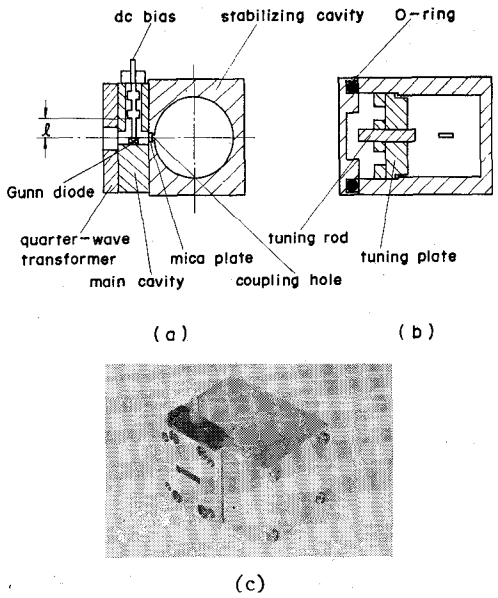

Fig. 1. (a) Cross section of stabilized K_a-band Gunn oscillator. (b) Cross section of stabilizing cavity. (c) Photograph of oscillator.

by coupling a high-Q cavity to the oscillator. There are many methods of coupling. The most useful method is to couple a reaction cavity directly to the oscillator [1], [2], because the power loss due to the stabilization is only 1 dB or less, theoretically and experimentally [3]. This correspondence describes a highly stabilized K_a-band Gunn oscillator. Experimental results on the frequency-saturation effect [4], [5] are also described.

The construction and photograph of the K_a-band Gunn oscillator are shown in Fig. 1. The main cavity is made of a waveguide-coaxial microwave circuit in which the upside-up Gunn diode, having the impurity concentration of 1×10^{15} cm^{-3} and the active-layer thickness of 6 μ, is imbedded. The dimension of the waveguide cross section is 2×8.6 mm. The cavity is coupled to the standard waveguide WRJ-260 (in Japan) through a quarter-wave transformer to make the circuit conductance equal to the value G_1, at which maximum generation power can be obtained. The stabilizing cavity operating in the cylindrical TE_{011} mode is made of a "super-invar" whose thermal expansion coefficient α is about 5×10^{-7}/°C, and is hermetically sealed by means of a micaplate and an Oring to prevent the intrusion of moisture (Fig. 1). The temperature coefficient of the resonant frequency of the cavity $\Delta f/f_0$ is given by

$$\frac{\Delta f}{f_0} = -\alpha\left(1-\frac{3}{2}\frac{\epsilon_r-1}{\epsilon_r}\right)\ ^\circ\mathrm{C}^{-1}$$

where f_0 and ϵ_1 are the resonant frequency of the cavity and the relative dielectric constant of the medium filling the cavity, respectively. The assumption is made that the cavity is filled with dry air. The temperature coefficient is nearly equal to $-\alpha$, because the second term in the parenthesis is negligibly small as compared with unity.

The resonant frequency of the main cavity f_1, or the oscillation frequency of the oscillator when the coupling coefficient k is zero, can be adjusted by varying the length of the coaxial circuit l. The frequency f_1 can also be adjusted by means of a short plunger in the waveguide (not used in the oscillator shown in Fig. 1). The highest oscillation frequency f_H in the oscillator is restricted by the frequency-saturation effect and the mode switching [4], [5]. One of the reasons is as follows. The load conductance at device terminals increases with the increase of frequency, provided that the series resonant frequency f_s of the packaged device is lower than the frequency range of interest [6]. In order to increase f_H, we have to increase f_s. This can be achieved by reducing the series inductance of the diode package.

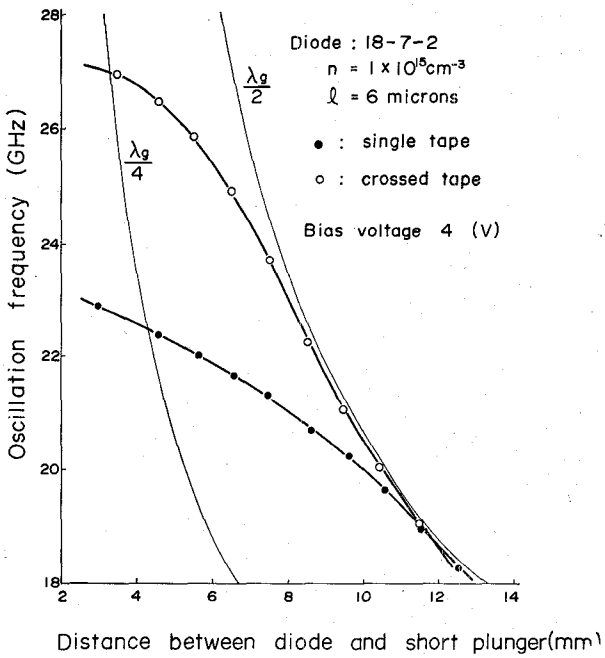

Fig. 2. Tuning characteristics in unstabilized oscillators using a single-tape diode and crossed-tape diode. Impurity concentration is 1×10^{15} cm^{-3}, and active-layer thickness is 6 μ.

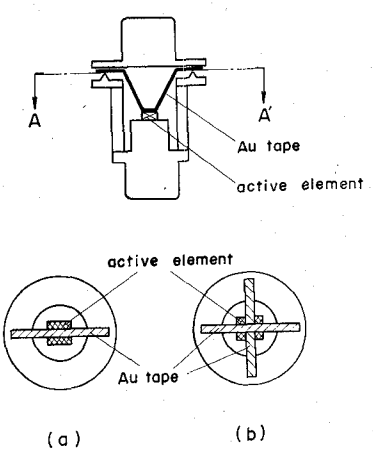

Fig. 3. Typical cross section of diode package. (a) Single-tape diode. (b) Crossed-tape diode.

The tuning characteristics of the unstabilized oscillator, made of a reduced-height k-band waveguide, are shown in Fig. 2. Dots and circles show the experimental results obtained in the oscillators using a single-tape and a crossed-tape diode, respectively. The two diodes are schematically shown in Fig. 3.

By use of a crossed-tape diode, the tuning range from 22 to 28 GHz has been obtained by adjusting l (see Fig. 1). The distance between the diode and the coupling hole is a quarter-wavelength at 25 GHz, and the stabilizing cavity is detuned. Typical tuning characteristics for a fixed f_1 are shown in Fig. 4 as a function of f_0, where the coupling coefficient k is 3.7×10^{-3}, Q_1 (external Q of the main cavity) $=10$, Q_0 (unloaded Q of the stabilizing cavity) $=15\,000$, and f_1 $=24.61$ GHz. The results show that the differential susceptance with the negative conductance dB_d/dG_d ($G_d<0$) or $\tan\theta$ (gradient of the diode-admittance locus for a fixed frequency in the susceptance–conductance plane) is positive, as in the IMPATT diode [1], and that the f_+ mode (Fig. 4) is more preferable than the f_- mode for stabilization. It should, however, be noticed that the other case exists in the Gunn diode. According to the results of computer simulation, $\tan\theta$

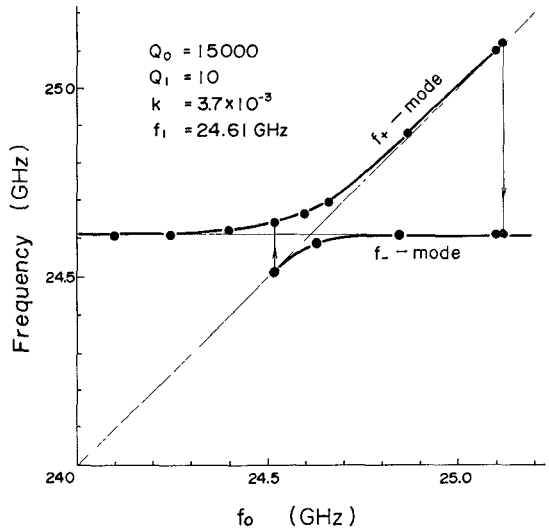

Fig. 4. Typical tuning characteristic of stabilized K_a-band Gunn oscillator as a function of f_0.

TABLE I
EXPERIMENTAL RESULTS

Operating frequency	25.01 GHz
output power	30 mW
Pushing figure	-0.7 KHz/mV
Frequency stability	-6×10^{-7} °C^{-1}
Bias voltage	-4 V
Dc current	500 mA

is negative at a frequency somewhat higher than the transit-time frequency f_T of the diode [7], [8]. We can obtain the condition $\tan\theta > 0$ by decreasing the bias voltage V_0. The frequency f_T increases as V_0 decreases if the diode has the impurity concentration which is higher at the anode than at the cathode side [9]. In order to prevent mode jumping, the difference of the two frequencies $\Delta f(=f_0-f_l)$ should be smaller than the critical value [1], [2], which is 400 MHz in this oscillator. The results obtained in the stabilized oscillator are listed in Table I, where $\Delta f=400$ MHz. The frequency stability of 3×10^{-5} has been obtained over the temperature range from 0 to 50°C. The power loss has been minimized by adjusting the characteristic impedance of the transformer, and making the load conductance at $k=0$ smaller than G_l [3]. The output power at $k=3.7\times10^{-3}$ was only 0.5 dB lower than the maximum generation power at $k=0$ and $f=25$ GHz. The frequency stability against the variation of the bias voltage is lower than 3×10^{-3}/mV. The oscillator can be operated in the frequency range up to 30 GHz by modifying the dimensions of the cavities. An output power of more than 20 mW has been obtained.

ACKNOWLEDGMENT

The authors wish to thank Y. Aono for the preparation of the Gunn diodes, H. Kondo and T. Itano for their help in experimental work, and Dr. H. Murakami, Dr. K. Ayaki, and Dr. K. Sekido for their encouragement and guidance.

REFERENCES

[1] S. Nagano and H. Kondo, "Highly stabilized half-watt IMPATT oscillator," *IEEE Trans. Microwave Theory Tech. (Special Issue on Microwave Circuit Aspects of Avalanche-Diode and Transferred Electron Devices)*, vol. MTT-18, pp. 885–890, Nov. 1970.
[2] Y. Itoh, H. Komizo, and S. Sasagawa, "Cavity stabilized X-band Gunn oscillator," *IEEE Trans. Microwave Theory Tech. (Special Issue on Microwave Circuit Aspects of Avalanche-Diode and Transferred Electron Devices)*, vol. MTT-18, pp. 890–897, Nov. 1970.
[3] S. Nagano, "Stabilization of solid-state microwave oscillator by means of a reaction cavity—Stabilization factor and power loss," *Trans. Inst. Electr. Commun. Eng. Japan*, vol. 54-B, pp. 286–288, May 1971.
[4] B. C. Taylor, S. J. Fray, and S. E. Gibbs, "Frequency-saturation effects in transferred electron oscillators," *IEEE Trans. Microwave Theory Tech. (Special Issue on Microwave Circuit Aspects of Avalanche-Diode and Transferred Electron Devices)*, vol. MTT-18, pp. 799–807, Nov. 1970.
[5] W. C. Tsai, F. J. Rosenbaum, and L. A. MacKenzie, "Circuit analysis of waveguide-cavity Gunn-effect oscillator," *IEEE Trans. Microwave Theory Tech. (Special Issue on Microwave Circuit Aspects of Avalanche-Diode and Transferred Electron Devices)*, vol. MTT-18, pp. 808–817, Nov. 1970.
[6] S. Furukawa and S. Horiguchi, "Load characteristics of Read type avalanche diode," *Trans. Inst. Electr. Commun. Eng. Japan*, vol. 52-C, pp. 735–742, Nov. 1969.
[7] S. Nagano, "Stabilization of microwave solid-state oscillators with a reflection cavity," *Papers Tech. Group Microwaves*, IECEJ, Dec. 1969.
[8] S. Nagano and M. Suga, "Large-signal analysis of a Gunn diode oscillator for circuit design," *Papers Tech. Group Microwaves*, IECEJ, Apr. 1971.
[9] M. Suga and K. Sekido, "Effect of doping profile upon electrical characteristics of Gunn diodes," *IEEE Trans. Electron Devices*, vol. ED-17, pp. 275–281, Apr. 1970.

Broad-Band Parametric Amplifier Design

G. R. BRANNER, E. R. MEYER, AND P. O. SCHEIBE

***Abstract*—A computerized optimization technique is employed to provide design values for broad-band parametric amplifiers. Some results of the procedure are presented.**

Parametric amplifiers are of primary importance for design of low-noise microwave receivers. The importance of broad-band low-noise parametric amplifiers for use in satellite communication systems has been reemphasized recently [1], [2]; and it has also been suggested that frequencies above 10 GHz are quite attractive for commercial satellite systems since they are not so heavily utilized. In the past, bandwidths as high as 20 percent (for 20-dB gain stages) have been obtained at lower frequencies; however, at frequencies above X band, considerably smaller bandwidths have been reported.

It is the objective of this correspondence to present the results obtained from a computer-oriented optimization technique which is capable of providing realizable designs for extremely wide-band parametric amplifiers (40-percent 3-dB bandwidths have been obtained at low K band). The optimization procedure employs the Gauss–Newton iteration technique (requiring exact evaluation of all the essential partial derivatives of the objective function [3], [4]).

As is well known, the variation of parametric amplifier gain with respect to frequency is strongly dependent on the form of tuned circuits at signal and idler frequencies, and considerable effort has been expended toward the development of analytical techniques for selecting resonator parameter values to provide broad bandwidth [5]–[7].

The approach described in this correspondence is to utilize a prescribed amplifier topology (triple-tuned signal and single-tuned idler circuits) and employ computerized optimization to obtain realizable matching network element values which provide maximally flat bandwidths.

The nondegenerate parametric amplifier configuration which was employed is illustrated in Fig. 1(a). The varactor model [Fig. 1(b)] includes parasitic case capacitance (C_p), series lead inductance (L_0), and internal resistance (R_0). It was also assumed that signal and idler circuits are isolated by ideal bandpass filters centered, respectively, in the signal and idler bands of interest.

The mathematical model for the amplifier was developed using standard analytical techniques (see [8] for example):

Manuscript received March 23, 1971; revised September 19, 1971.
G. R. Branner is with ESL Incorporated, Sunnyvale, Calif. 94086.
E. R. Meyer and P. O. Scheibe were with ESL Incorporated, Sunnyvale, Calif. 94086; they are now with ADAC Incorporated, Sunnyvale, Calif.